Coupled Anthraquinone and Glutathione Control of Tellurite Bio-Removal and Tellurium Nanoparticles Bio-Synthesis

Rui Zhao[1+], Weihong Zhang[1+], Yuanyuan Song[1*], Haibo Li[1], Zhi Chen[2], Ya-nan Hou[1], Caicai Lu[1], Yi Han[1], Daohong Zhang[1], Jianbo Guo[1*]

[1]School of Environmental and Municipal Engineering, Tianjin Key Laboratory of Aquatic Science and Technology, Tianjin Chengjian University, Jinjing Road 26, Tianjin 300384, China

[2]Department of Building, Civil, and Environmental Engineering, Concordia University, 1455 de Maisonneuve Blvd. W. Montreal, Quebec, Canada

[+]Co-first author.

*Corresponding Author.

Abstract:

This study focuses on bio-removal of highly toxic tellurite (Te(IV)) by producing biological tellurium nanoparticles (Bio-TeNPs) under anaerobic conditions. The coupled Anthraquinone and Glutathione (AQDS@GSH) was novelly proposed to increase Te(IV) bio-removal rate 4.7-fold by *S.oneidensis* MR-1. Meanwhile, distinguishing features of the Bio-TeNPs were characterized by Zeta potential, Dynamic Light Scattering (DLS), FT-IR spectroscopy and TEM, which were covered with more abundant extracellular secretion and distinguish from the original. Moreover, the Michaelis-Menten fitting suggested that was a stronger bond ($Km^{-1}_{AQDS@GSH}$= 9.212 $L \cdot mg^{-1}$> Km^{-1}control = 0.0173 $L \cdot mg^{-1}$) between Te(IV) and Te(IV) reductase. Since AQDS was added value to electron transfer and balance the Oxidation-Reduction pressure, GSH was introduced to direct the size and shape of the Bio-TeNPs. Therefore, the coupled AQDS@GSH biosystem contributed to coupled effect, which was proved and quantified by Coupled Factor Evaluation (1.2>1.0). This study provides the coupled strategy for potentially toxic metal biotreatment and improves feasibility for recovery of scarcity metal.

Keywords: Tellurite; Bio-TeNPs; AQDS@GSH; coupled effect; S. oneidensis MR-1.

I. INTRODUCTION

Tellurium pollution in environment have been increased with the widespread use in industrial production of medicine, rubber, glass, solar panels, aerospace equipment, and mining operations. Especially, highly oxidation states such as tellurite (Te(IV)) and tellurate (Te(VI)) rendered acute toxicity to public health and wildlife[1-2], prompting demand for the effective control of tellurium pollution in the environment. Among these oxidation states, Te(IV) is soluble and the most toxic to living organisms. Despite high toxicity of Te(IV), several microorganisms could resist and reduce Te(IV) via synthesis of insoluble,amorphous, and less toxic biological tellurium nanoparticles (Bio-TeNPs) under anerobic or aerobic conditions. Moreover, the biosynthetic nanoparticles with well-defined size and high surface areas frequently exhibited

extraordinary catalytic, antimicrobial, and photoconductive properties, while its nanostructures were largely influenced by microbial activities and biosynthetic process[3-4]. For example, the structure and size of Bio-TeNPs can be controlled by environmental conditions (pH, temperature, reaction time, etc.)[5], and the Bio-TeNPs synthesized by *S. baltica*GUSDZ9 exhibited excellent photo-catalytic properties for methylene blue and anti-biofilm activities. Therefore, microbial treatment is not only an effective method to reduce highly toxic Te(IV), but also a potential approach to produce and recycle applicable Bio-TeNPs[6].

Nevertheless, in recent years, the wide application of nano materials was extremely limited by the structural relaxation effect on nanocrystalline, such as aggregation and aging. Therefore, the shape and size of Bio-TeNPs should be prioritized to regulate and control during the synthesis process for maintaining the demand-satisfying physicochemical properties. It was reported that GSH can stabilize the structure of aged quantum colloids and rejuvenate the luminescent property[7], which also played an important role as an antioxidant and detoxification agent for biological potentially toxic metal reduction and nanoparticles synthesis[8-9]. Therefore, GSH can be considered to control the size of Bio-TeNPs for large-scale application. However, it seemed that the tough challenge isboostingbioreduction efficiency, simultaneouslyreclaiming validBio-TeNPs.

Previous studies reported that the quinones (AQS, AQDS, etc.) can accelerate the biotransformation efficiency of pollutants with excellent redox reversibility and desirable biocompatibility[10]. The quinones can transform reversibly along with redox state conversion for accelerating electron transfer efficiencies of biotransformation. In addition, the quinones can also promote extracellular nanoparticles synthesis. Therefore, the quinones were considered for accelerating and controlling Bio-TeNPs synthesis. But regulatory effect and mechanism of quinones on structure and properties of Bio-TeNPs need to be explored in detail. Moreover, it was reported that Fe(III) and AQDS synergistically could enhance Cr(VI) bioreduction rate, which provided a potential synergy and coupled strategy between quinones and GSH for Bio-TeNPs synthesis on theoretical level[10]. However, the knowledge of acting mechanism between the quinones and GSH on Bio-TeNPs synthesis in microorganisms is very limited. The hypothesis was raised that the combined effect of the coupled quinones and GSH would accelerate the Bio-TeNPs synthesis. Such knowledge is particularly important for developing highly effective nanotechnology for simultaneously attaining Te(IV) bio-removal and Bio-TeNPs synthesis.

This study aims to investigate the coupled effects and potential mechanism between quinones and GSH on Te(IV) bio-removal, Bio-TeNPs synthesis and characterize the synthetic Bio-TeNPs properties. In this study, *S. oneidensis* MR-1 was chosen as the model dissimilatory metal reduction bacteria since it has been studied intensively for potentially toxic metalbioreduction[11]. And the optimal quinone was filtered out (details were shown by pre-experiment in section of materials and methods), meanwhile the accelerating effect of quinone and GSH on Bio-TeNPs synthesis in MR-1 was evaluated. Besides, the physicochemical properties of Bio-TeNPs were characterized by several methods (Transmission Electron Microscope UV–vis, Zeta potential, Fourier Transform Infrared (FT-IR), fluorescence spectra). Moreover, the potential mechanism between quinones and GSH on Bio-TeNPs synthesis was explored by redox potential (ORP), GSH level in MR-1, size analysis, Michaelis-Menten fitting and Coupled factor evaluation.

II. MATERIALS AND METHODS

2.1 Microorganism enrichment and culture conditions

S. oneidensis MR-1 in this study was obtained from Ocean Microbial Culture Collection of China and preserved at -80 ℃. It was pre-cultured 10 h using Luria-Bertani medium (35 ℃, pH 7.0, 140 rpm·min^{-1}) to logarithmic phase. The biomass was incubated in serum bottles (150 mL) until the Optical Density reached 1.0 at 600 nm. Then Te(IV) bioreduction was performed in anaerobic conditions (35 °C, pH 8.0), which consisted of components following previous report[11]. Sodium lactate (20 mmol· L^{-1}) was supplied as carbon source.

2.2 The optimization of quinones varieties on Te(IV) bio-removal

Previous research, Anthraquinone-2-sulfonate (AQS), Anthraquinone-1-sulfonate (α-AQS), Anthraquinone-1,5-disulfonate (1,5-AQDS), and Anthraquinone-2,6-disulfonate (AQDS) at same quantity at 0.2 mmol·L^{-1} was added respectively. The highest reduction rate was exhibited by AQDS (77%) compared with others (AQS 69%, α-AQS 62%, 1,5-AQDS 41%). Therefore, AQDS was elected as the prior quinone for following studies. Meanwhile, chemical control was experimented to eliminate abiotic effect.

2.3 The acceleration of Te(IV) bio-removal by coupled AQDS@GSH

Batch experiments were conducted which contained the GSH chem-reduction system (0.4 mmol·L^{-1} GSH and 0.1 mmol·L^{-1} Te(IV)), control system (MR-1 bacterial suspension, sodium lactate, and 0.1 mmol·L^{-1} Te(IV)), GSH supplemented system (MR-1 bacterial suspension, sodium lactate, 0.4 mmol·L^{-1} GSH and Te(IV)), AQDS supplemented system (MR-1 bacterial suspension, sodium lactate, 0.2 mmol·L^{-1} AQDS and Te(IV)), and AQDS@GSH supplemented system (MR-1 bacterial suspension, sodium lactate, AQDS@GSH and Te(IV)). The concentration of components in each system keeps same. All bottles were sealed after repeatedly blowing off by nitrogen gas. The results present averages of experiments in triplicate, and error bars represent standard deviations.

2.4 Determination of GSH concentration in MR-1

The MR-1 cells were collected, centrifuged (10,000 rpm·min^{-1}, 10 min, 4 °C) and resuspended in PBS buffer (pH 7.4). Then the cells were disrupted by freeze-thaw and separated by centrifugation (20,000 rpm·min^{-1}, 15 min, 4 °C) to obtain the supernatant for determining the GSH concentration, which was determined by GSH Assay Kit (Beyotime Instituted of Biotechnology, China). And the GSH concentration were detected by Microplate Reader (VEDENG Technology, China) and calculated per gram of cell concentration[12].

2.5 Characterization of Bio-TeNPs

The ORP was determined by redox online analyzer (PURA22, JULABO RTKINS, China), Bio-TeNPs liquid was utilized to measure Zeta potential and DLS in PBS buffer at pH 3.0−10.0 by Zeta potential

Analyzer (Nano ZS, Malvern, USA). The MR-1 cells were collected for detecting Bio-TeNPs synthesis by TEM. Samples were fixed in glutaraldehyde PBS (2.5%, pH 7.4), and serially dehydrated with 30%, 50%, 70%, 85%, 95%, 100% ethanol. The images were obtained at 120 kV by TEM (H7650, HITACHI, Japan). A fluorescence microscope (IX51, Olympus, Japan) and FT-IR spectrometer (Nicolet Is10, Thermo Fisher, USA) was used to determine the morphology and function groups of Bio-TeNPs.

2.6 The kinetics of the Michaelis-Menten and Coupled factor equation

The kinetic rates of Te(IV) bio-removal can be describedby the Michaelis-Menten equation (1):

$$v = \frac{V_{max}\,[S]}{K_m + [S]} \tag{1}$$

where$v$represents the Te(IV) bio-removal rate (mg·L^{-1}·h^{-1}), V_{max} represents the maximum Te(IV) bio-removal rate (mg·L^{-1}·h^{-1}), [S] represents the Te(IV) concentration (mg·L^{-1}), and K_m represents the Michaelis-Menten constant (mmol).

The coupled factor was defined as equation (2) for quantifying the coupled effect of AQDS and GSH[13-14]:

$$\text{Coupled factor} = \frac{v_{AQDS\,@GSH}}{v_{AQDS} + v_{GSH}} \tag{2}$$

where v represents Te(IV) bio-removal rate (mg·L^{-1}·h^{-1}), if coupled factor ≥ 1.0, it means coupled effect, if coupled factor ≤ 1.0, it means no coupled effect.

2.7 Analytical methods

The Bio-TeNPs were detected by UV-vis (Shimadzu 2600, Japan)at 190-450 nm. Samples (1.5 mL) were collected regularly centrifuged at 10,000 rpm·min-1, 4 °C for 10 min. Then the supernatant was diluted with 1% HNO$_3$ and determined by ICP-MS (Agilent 7700e, USA) for Te(IV) concentration analysis.

III. RESULTS AND DISCUSSION

3.1 The accelerating effect on Te(IV) bio-removal by coupled AQDS@GSH

Four different systems (control system, GSH supplemented system, AQDS supplemented system, and AQDS@GSH supplemented system) were set to further investigate the coupled effects of AQDS@GSH on Te(IV) bio-removal. After 12 h, in the four systems, the corresponding Te(IV) bio-removal efficiencies were 30%, 52%, 77%, and 96%, respectively (Fig1). It can be shown a higher Te(IV) bio-removal efficiency was attained with AQDS@GSH. And the chemical reduction by GSH can be ignored with the Te(IV) bio-removal efficiency of only 6%. A phenomenon of slight chemical reduction by GSH was probably due to the sulfhydryl group (-SH) of GSH could reduce heavy metals as a reductant[15]. However, a higher Te(IV) bio-removal efficiency in control system compared to the chemical reduction by GSH suggested that GSH played a significant role on Te(IV) bioreduction in cells[16]. It was commonly studied that Te(IV) reductase in the cells can accelerate conversion between GSSG and GSH for improving electron transfer efficiency[17]. In brief, the coupled AQDS@GSH can deeply accelerate Te(IV) removal with MR-1.

Furthermore, the possible coupled mechanism of AQDS@GSH on Bio-TeNPs synthesis was investigated in detail as followed.
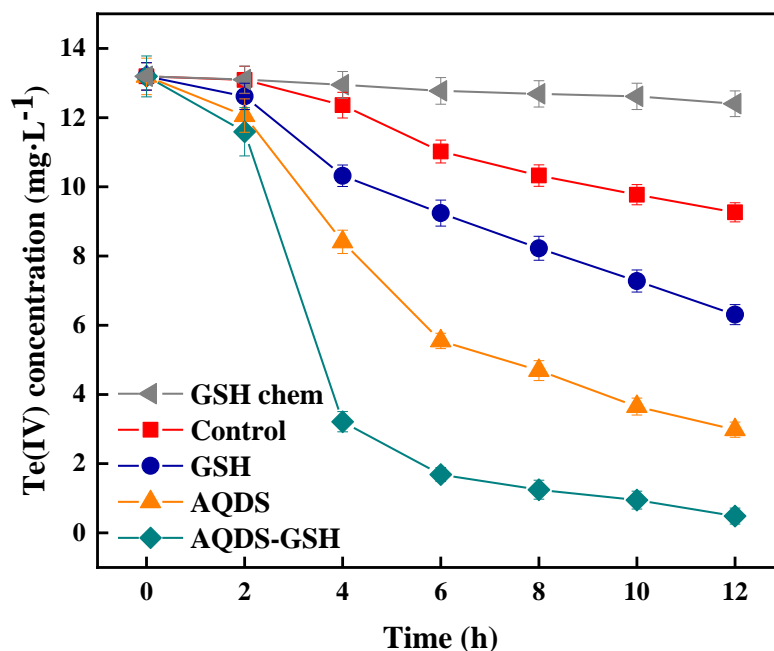

Fig1:The accelerating effect on Te(IV) bio-removal

3.2 Coupled mechanism of AQDS@GSH on Bio-TeNPs synthesis

Based on the acceleration effect of coupled AQDS@GSH on Te(IV) bio-removal, the coupled mechanism of AQDS@GSH on Bio-TeNPs synthesis was further studied in Fig2. As shown in Fig2a, the ORP in four systemswithin 24 h declined and stabilized at -218 mV, -212 mV, -341 mV, and -385 mV, corresponding to the control system, GSH supplemented system, AQDS supplemented system and AQDS@GSH supplemented system, respectively. Compared with GSH supplemented system and AQDS supplemented system, it can be shown that AQDS has givensignificant contribution to ORP decrease andreductive environment during Bio-TeNPs synthesis. As for aspect of electron transfer, it was reported that Te(IV) bioreduction in cells through the conversion between GSH and GSSG (oxidized glutathione), the redox potentials of AQDS ($E^{0'}$(AHQDS/AQDS)= -184 mV) are between $E^{0'}$(GSH/GSSG)= -240 mV and $E^{0'}$(Te(IV)/Te(0))= +827 mV, which allows AQDS can theoretically accelerate electron transfer efficiencies of conversion between GSH and GSSG during Bio-TeNPs synthesis[10]. For further proving the effect of AQDS on conversion between GSH and GSSG, the GSH level in MR-1 was shown in Fig2b. During 0 h-12 h, the GSH level in MR-1 was stabilized at 69.35 nmol·g^{-1}/cell, maintaining a steady-state redox balance in cells. Nevertheless, afterthe addition of Te(IV), the GSH level was sharply decreased to 7.80 nmol·g^{-1}/cell, indicating that protection against oxidative stress caused by Te(IV) via GSH consumption. On the contrary, afterthe addition of Te(IV)+AQDS, GSH consumption was gradually turned weaklyand stabilized at 12.28 nmol·g^{-1}/cell eventually, which suggested that AQDS probably promoted the conversion between GSSG and GSH.On the other hand, GSH controlled of Bio-TeNPs synthesis with an average particle size below 100 nm

and even a much smaller size formed by AQDS@GSH(Fig2c). Therefore, compared with AQDS, GSH can not only be considered as an antioxidant and detoxification agent in organisms, but also have effect on controlling the Bio-TeNPs size mainly[8].

Moreover, in Fig2d, the kinetics of the Bio-TeNPs synthesis suitably fit the Michaelis-Menten model under the zero-order kinetics, which is consistent with previous studies[18]. As the equation (1), the K_m^{-1} values were 0.0173 L·mg^{-1}, 0.0441 L·mg^{-1}, 0.1766 L·mg^{-1}, and 9.212 L·mg^{-1} for the control, GSH, AQDS, and AQDS@GSH supplemented system respectively. A higher K_m^{-1} value of the AQDS@GSH supplemented system suggested that AQDS@GSH enhanced the electron transfer efficiencies by distinctly strengthening the bond between Te(IV) and Te(IV) reductase. This converted the Bio-TeNPs synthesis into a molecular electron transfer reaction[11]. The Coupled factor was evaluated as equation (2) for further studying the coupled mechanism of AQDS@GSH on Bio-TeNPs synthesis. The Te(IV) bio-removal rate of control, GSH, AQDS, AQDS@GSH supplemented systems were 0.366 mg·L^{-1}·h^{-1}, 0.543 mg·L^{-1}·h^{-1}, 0.914 mg·L^{-1}·h^{-1}, 1.719 mg·L^{-1}·h^{-1}, respectively. The Te(IV) bio-removal rates of AQDS@GSH increased 4.7-fold compared with the control system, and the coupled factor was 1.2 greater than 1.0, indicating the coupled effect during Te(IV) bio-removal process.

In summarize, in the coupled AQDS@GSH, AQDS made a major contribution to reductive environment, meanwhile, GSH was conducive to shrink and brightenthe Bio-TeNPs. Furthermore the coupled AQDS@GSH strongly strengthened the bond between Te(IV) and Te(IV) reductase by Michaelis-Menten fitting, furthermore, the coupled effect of AQDS@GSH on Te(IV) bio-removal was quantified by Coupled factor evaluation (Fig2e).
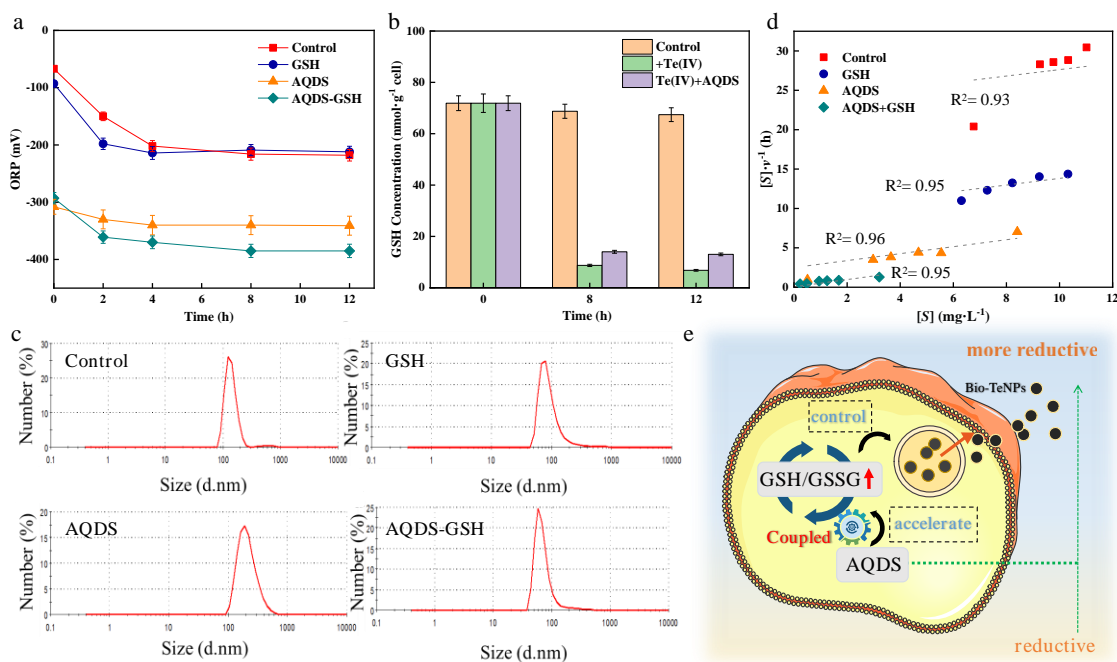

Fig. 2: ORP variation (a), GSH concentration in MR-1(b), size analysis (c), Michaelis-Menten fitting (d), coupled mechanism of AQDS@GSH (e)

3.3 Bio-TeNPs properties and potential application prospect

For details on characterizing Bio-TeNPs controlled by coupled AQDS@GSH, the surface characteristics of Bio-TeNPs were shown in Fig3. The Bio-TeNPs, black nanorods, were dispersed both in the intracellular and extracellular cells (Fig3a). It was proved the Bio-TeNPs synthesis by UV-vis spectrum which showed a maximum absorption peak at 210 nm (Fig3b). Organic layers are usually covered on the surface of nanoparticles, which affect the surface properties and stability[19]. Therefore, the Zeta potential of Bio-TeNPs were measured for studying the effect of AQDS@GSH on surface charge of Bio-TeNPs. In Fig3c, with the pH increasing, the Zeta potential of Bio-TeNPs was decreased from 17.363 mV to -32.913 mV and from 20.833 mV to -21.353 mV in the control and AQDS@GSH supplemented systems, which was consistent with previous studies[1]. Stronger electronegativity and stability were shown after AQDS@GSH addition, suggesting negatively charged functional groups were generated. FT-IR spectroscopy was determined to detect functional groups on surface of Bio-TeNPs (Fig3d). The peak at 1057 cm^{-1} are attributed to C—O—C representing the polysaccharides generation. And the peaks at 1220 cm^{-1}, 1430 cm^{-1} and 1390 cm^{-1} are attributed to P=O and —O—C=O stretching vibration. The peaks between 3000 to 3500 cm^{-1} are attributed to =C—H and N—H stretching vibrations, the peaks at 2920 cm^{-1} are attributed to C—H stretching vibrations in coating proteins, and the amide I and II band are observed at 1650 cm^{-1} and 1536 cm^{-1}[20].

Based on the distinguishing feature above, AQDS@GSH mightoptimize substanceand ingredient ofthe coating proteins, resulting in controlling the size of Bio-TeNPs(Fig2c).In fact, the properties of nanomaterials are dependent on their size and shape because of the large surface and volume ratio. Biological nanomaterials with a defined size had high antibacterial activity for drinking water disinfection, providing an attractive application prospect for Bio-TeNPs. In addition, it was interesting to note that the coating proteins actually promote the Bio-TeNPs stability andfluorescence property for further (Fig3e), which attributed to the coupled effect by AQDS@GSH. As a consequence, AQDS@GSH provided a novel method on controlling of Bio-TeNPs synthesis process and efficiency, even comprehensively expanding for Bio-TeNPs applications on emerging industry.
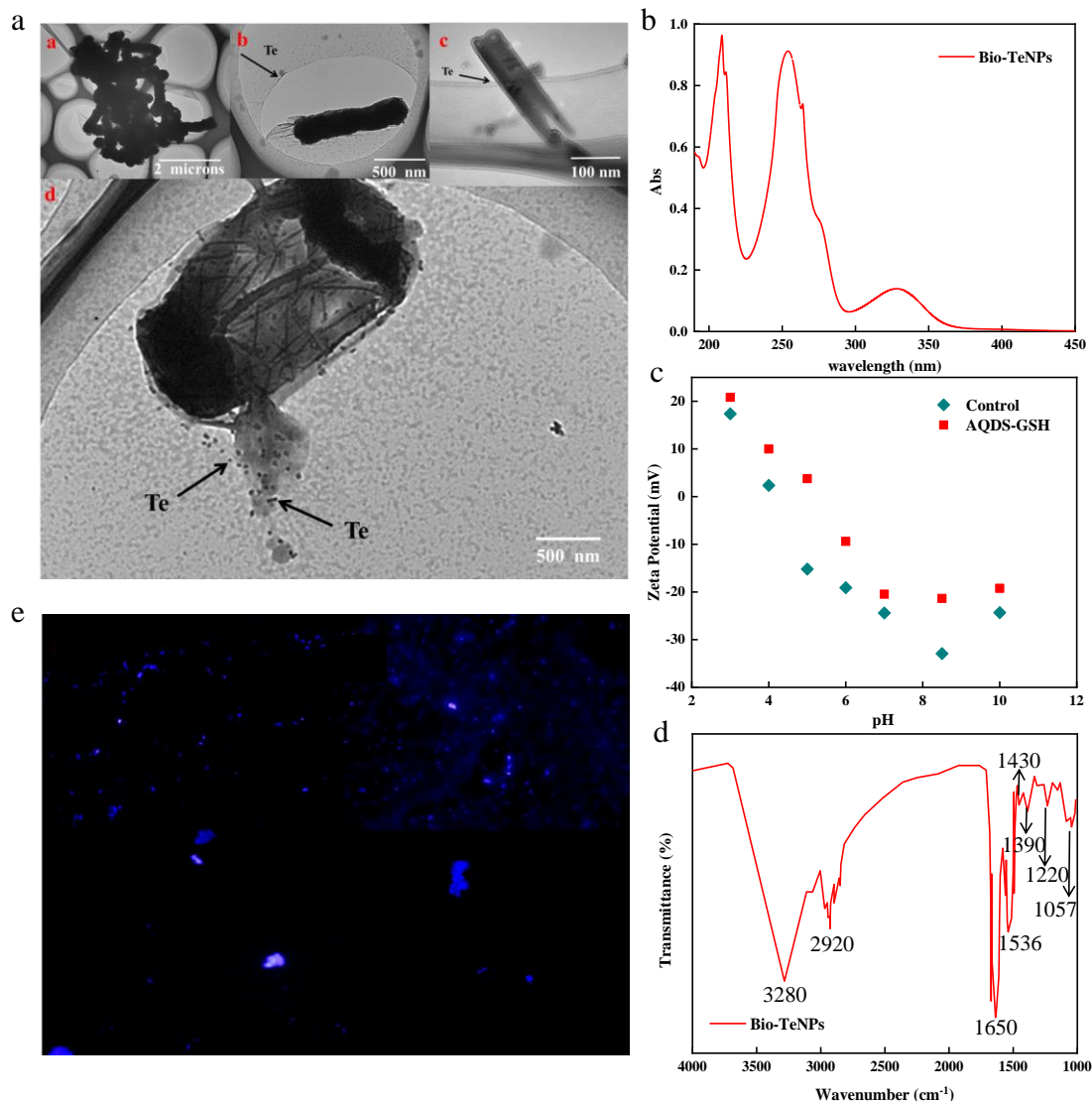
Fig3:TEM (a), UV-vis (b), Zeta potential (c), FT-IR (d), fluorescence (e) of Bio-TeNPs

IV. CONCLUSION

Tellurite (Te(IV) of highly toxic and strong oxidizingcould be effective bio-removal by adding AQDS@GSH.The Bio-TeNPs produced by coupled biosystem exhibited stronger electronegativity, stability and fluorescence property.The coupled effect was proved and quantified to explain underlying mechanism.Thisstudy provides antheoretical basis for investigating theTe(IV)biotreatment and further extended controllable Bio-TeNPs bio-synthesis for practicable application in the future.

ACKNOWLEDGEMENTS

REFERENCES

[1] He Y, Guo J, Song Y, Chen Z, Zhao R (2021) Acceleration mechanism of bioavailable Fe(Ⅲ) on Te(IV) bioreductionof Shewanellaoneidensis MR-1: Promotion of electron generation, electron transfer and energy level. Journal of Hazardous Material403:123728

[2] He Q, Yao K (2011) Impact of alternative electron acceptors on selenium(IV) reduction by Anaeromyxobacterdehalogenans. Bioresource Technology 102:3578-3580

[3] Plaza DO, Gallardo C, Straub YD, Bravo D, Perez-Donoso JM (2016) Biological synthesis of fluorescent nanoparticles by cadmium and tellurite resistant Antarctic bacteria: exploring novel natural nanofactories. Microbial Cell Factories 15:76

[4] Liang X, Perez MAM, Zhang S, Song W, Armstrong JG, Bullock LA, Feldmann J, Parnell J, Csetenyi L, Gadd GM (2020) Fungal transformation of selenium and tellurium located in a volcanogenic sulfide deposit. Environmental Microbiology 22:2346-2364

[5] Orizola J, Ríos-Silva M, Muñoz-Villagrán C, Vargas E, Vásquez C, Arenas F (2020) In vitro biosynthesis of Ag, Au and Te-containing nanostructures by Exiguobacterium cell-free extracts. BMC Biotechnology 20:29-34

[6] Wu S, Li T, Xia X, Zhou Z, Zheng S, Wang G (2019) Reduction of tellurite in Shinella sp. WSJ-2 and adsorption removal of multiple dyes and metals by biogenic tellurium nanorods. International Biodeterioration and Biodegradation 144:104751

[7] Bellacanzone C, Tarpani L, Gentili PL, Latterini L (2020) Effects of glutathione on the luminescent behavior of CdSe-nanocrystals. J Lumin. 226:117513

[8] Wang D, Xia X, Wu S, Zheng S, Wang G (2019) The essentialness of glutathione reductase GorA for biosynthesis of Se(0)-nanoparticles and GSH for CdSe quantum dot formation in Pseudomonas stutzeri TS44. Journal of Hazardous Material 366:301-310

[9] Dou X, Dai H, Twardowska I, Wei S(2020) Hyperaccumulation of Cd by Rorippaglobosa (Turcz.) Thell. from soil enriched with different Cd compounds, and impact of soil amendment with glutathione (GSH) on the hyperaccumulation efficiency. Environmental Pollution 255:113270

[10] Li H, Guo J, Jing L, Zhao L, Yang J (2013) Effective and characteristics of anthraquinone-2,6-disulfonate (AQDS) on denitrification by Paracoccusversutussp GW1. Environmental Technology 34:2563-2570

[11] Zhao R, Guo J, Song Y, Chen Z, Lu C (2020) Mediated electron transfer efficiencies of Se(IV) bioreduction facilitated by meso-tetrakis (4-sulfonatophenyl) porphyrin. International Biodeterioration and Biodegradation 147:104838

[12] Wang G, Wang H, Xiong X, Chen S, Zhang D (2015) Mitochondria thioredoxin's backup role in oxidative stress resistance in Trichodermareesei. Microbiology Research 171:32-38

[13] Weng CH, Lin YT, Yuan HM (2013) Rapid decoloration of Reactive Black 5 by an advanced Fenton process in conjunction with ultrasound. Separation and Purification Technology 117:75-82

[14] Zhou T, Wu X, Zhang Y, Li J, Lim TT (2013) Synergistic catalytic degradation of antibiotic sulfamethazine in a heterogeneous sonophotolytic goethite/oxalate Fenton-like system. Applied Catalysis B: Environmental 136:294-301

[15] Jozefczak M, Remans T, Vangronsveld J, CuypersA(2012) Glutathione Is a Key Player in Metal-Induced Oxidative Stress Defenses. International Journal of Molecular Science 13:3145-3175

[16] Luque-Garcia JL, Cabezas-Sanchez P, Camara C (2013) Analytical and bioanalytical approaches to unravel the selenium–mercury antagonism: A review. AnalyticaChimicaActa 801:1-13

[17] Rigobello MP, Folda A, Citta A, Scutari G, Gandin V, Fernandes AP (2011) Interaction of selenite and tellurite with thiol-dependent redox enzymes: Kinetics and mitochondrial implications. Free Radical Biology and Medicine 50:1620-1629

[18] Nguyen VK, Nguyen TH, Ha MG, Kang HY (2019) Kinetics of microbial selenite reduction by novel bacteria isolated from activated sludge. Journal of Environmental Management 236:746-754

[19]Zhang X, Fan W, Yao M, Yang C, Sheng G(2020) Redox state of microbial extracellular polymeric substances regulates reduction of selenite to elemental selenium accompanying with enhancing microbial detoxification in aquatic environments. Water Research 172:115538

[20]Priyanka U, Akshay GKM, Elisha MG, Surya TB, Nitish N, Raj MB (2016) Biologically synthesized PbS nanoparticles for the detection of arsenic in water. International Biodeterioration and Biodegradation119:78-86